EUROPEAN ORGANIZATION FOR NUCLEAR RESEARCH

CERN-EP/86-02
9 January 1986

PRECISION MEASUREMENT OF STRONG INTERACTION ISOTOPE EFFECTS IN ANTIPROTONIC ^{16}O, ^{17}O, AND ^{18}O ATOMS

Th. Köhler, P. Blüm, G. Büche, A.D. Hancock, H. Koch, A. Kreissl,
H. Poth, U. Raich and D. Rohmann
Kernforschungszentrum Karlsruhe, Institut für Kernphysik
and
Institut für Experimentelle Kernphysik, Universität Karlsruhe, Karlsruhe, Fed. Rep. Germany

G. Backenstoss, Ch. Findeisen, J. Repond and L. Tauscher
Institute for Physics, University of Basle, Switzerland

A. Nilsson and S. Carius
Research Institute of Physics, Stockholm, Sweden

M. Suffert
Centre de Recherches Nucléaires, Strasbourg, France

S. Charalambus, M. Chardalas and S. Dedoussis
Department of Nuclear Physics, University of Thessaloniki, Thessaloniki, Greece

H. Daniel, T. von Egidy, F.J. Hartmann, W. Kanert and G. Schmidt
Physik Department, Technische Universität München, Munich, Fed. Rep. Germany

J.J. Reidy and M. Nicholas
Physics Department, University of Mississippi, University, Miss., USA

A. Wolf
CERN, Geneva, Switzerland

ABSTRACT

The strong-interaction effects in antiprotonic ^{16}O, ^{17}O, and ^{18}O atoms were measured at the CERN antiproton facility, LEAR. The shifts ϵ and the widths Γ of the 3d level were determined to be -112 ± 20 eV (^{16}O), -140 ± 46 eV (^{17}O), -195 ± 20 eV (^{18}O), and 495 ± 45 eV (^{16}O), 540 ± 150 (^{17}O), 640 ± 40 eV (^{18}O), respectively.

(Submitted to Physics Letters B)

1. INTRODUCTION

The determination of strong-interaction effects in exotic atoms is a proven technique for deriving the strong-interaction potential between a negatively charged hadron and the nucleus. Owing to the hitherto poor quality of secondary antiproton beams, strong-interaction effects have so far been measured for only a few antiprotonic atoms [1]. With the commissioning of the CERN Low-Energy Antiproton Ring (LEAR) [2] this situation has now changed considerably, enabling precision experiments to be carried out. As has been pointed out in an earlier publication [3], measurements of strong-interaction effects in light nuclei are particularly suitable for establishing the antinucleon–nucleus force. Moreover, by comparing strong-interaction effects in isotopes of the same element, information on the relative strength of the $\bar{p}p$ to the $\bar{p}n$ interaction can be obtained. In order to study these aspects, we have chosen the stable oxygen isotopes as targets in the first series of measurements at LEAR [4]. In the following we report on the measurement of the shifts and widths of the 3d level in ^{16}O, ^{17}O, and ^{18}O.

2. EXPERIMENTAL TECHNIQUE

The experimental set-up with its data-acquisition system has already been described [5]. As it will be discussed in more detail in a forthcoming report [6], we will give only a short summary here.

The experiment was set up in the M1 beam of LEAR. The incoming antiprotons of 300 MeV/c and 200 MeV/c, identified by two scintillation (telescope) counters, were moderated in a polyethylene block and stopped in the centre of the oxygen target. The target was a small container (4.5 cm × 4.5 cm × 0.3 cm) filled with water. Whilst the ^{16}O and ^{18}O were isotopically pure targets (purity > 99%), the ^{17}O was only enriched (^{16}O: 14.0%; ^{17}O: 61.9%; ^{18}O: 24.1%). The container consisted of an aluminium frame (3 mm thick) and beryllium foils (0.125 mm thick) which were glued onto each side of the frame. The whole assembly was placed in a helium bag to avoid contamination of the spectra from antiproton stops in air. Six solid-state detectors were mounted radially around the target. The energy and the time of arrival of each X-ray event were sorted into the memory of a microprocessor. A particular effort was made to carry out this procedure as quickly as possible [7]. Between the LEAR $\bar{p}$ spills (1 spill $\hat{=}$ 1 h beam time) the projected energy and time spectra were transferred to a PDP 11/35. The full two-dimensional spectra were also written on tape. Initial checking of the spectra was done on the PDP, which also monitored the count rates and recorded the moderator thickness. From the PDP the spectra were sent to a LSI 11/23 computer, where they were immediately analysed. The average antiproton rate was about $25 \times 10^3\ s^{-1}$.

The detectors were calibrated with radioactive sources before and after the run. For the evaluation of the strong-interaction effects, however, the oxygen lines unaffected by strong interaction were used to determine the in-beam energy and resolution calibration.

3. DATA EVALUATION AND RESULTS

The measured spectra (fig. 1) were nearly free of background and contained essentially oxygen lines with only a few aluminium transitions which stemmed from scattered antiprotons and annihilation pions stopping in the aluminium of the target frame and other structural elements. The X-ray cascade ended on the 3d level. Apart from the 4–3 transitions also 5–3 and 6–3 transitions, feeding the 3d level, were observed. In table 1 the numbers of stopped antiprotons and spills are shown for each target.

First the ^{16}O and ^{18}O spectra were analysed, spill by spill. All antiprotonic lines (except the 4–3 line) were fitted with triplets of Gaussians (transition between unresolved fine-structure levels) interlocked in width, relative intensity, and position on the basis of the pre-run source

calibration. From these fits an in-beam calibration of energy and resolution was obtained for each spill, using the unaffected oxygen lines. The energies of these lines were calculated with the program taking into account all relevant QED contributions [8]. Thereafter the 4–3 complex was fitted with three fully interlocked Lorentzians folded with Gaussians of fixed width (fig. 2). This analysis was complicated by the presence of the electronic K_α lines from lead (Pb) on each side of the 4–3 transition. The lines originated from minute lead impurities in materials used in the set-up. Particles coming from $\bar{p}$ annihilation in oxygen and penetrating the apparatus provoked this fluorescence, which appeared at the same time as the antiprotonic X-rays.

In the fits the relative intensity of the $K_{\alpha 1}$ and $K_{\alpha 2}$ lines was fixed, and only the intensity with respect to the 4–3 transition was varied. In this way the shift and the width for the 4–3 transition were determined separately for each spill and each detector. In table 2 the weighted mean of the three relevant detectors and of all single spills are given together with the total and the statistical errors. The latter is derived from the statistical error of the sum spectra. The systematic error is obtained by taking the one standard deviation width of the distribution generated by the results of the individual spills. The total error is the square root of the quadratic sum of statistical and systematic error.

Next the unperturbed antiprotonic X-ray lines in ^{17}O were fitted spill by spill, each line with three triplets accounting for the content of ^{16}O, ^{17}O, and ^{18}O in the target. The relative intensities of each triplet were fixed to the abundance of the isotopes. The Gaussian widths were taken equal and varied together. The relative position of each triplet was locked to the value given by the reduced mass energy shift ($^{18}E/^{16}E = 1.00664$; $^{17}E/^{16}E = 1.00351$). From these fits individual calibrations for each detector and each spill were derived. Thereafter, the 4–3 complex in ^{17}O was fitted (fig. 2) using the energy and Lorentzian width values obtained from the evaluation of the ^{16}O and ^{18}O spectra as a fixed input. The intensities of the ^{16}O and ^{18}O components were taken from the isotopic abundance and corrected for the different strong-interaction attenuation of the 4–3 transition in ^{16}O and ^{18}O, respectively. Again the ^{17}O component of the 4–3 complex was fitted with three lines corresponding to the transition between the unresolved fine-structure levels. We did not take into account a possible hyperfine splitting. The result of the ^{17}O evaluation is given in the second line of table 2. The systematic error is larger mainly because of the uncertainty of the strong-interaction effects in ^{16}O and ^{18}O.

4. DISCUSSION

The newly determined shifts and widths of the 3d level of antiprotonic ^{16}O and ^{18}O are in good agreement with our earlier measurements [3] (column 3 of table 3) and with the measurement of Barnes et al. [9] (column 4 of table 3). However, the new data are much more precise.

The isotope effect in the shift and width of the 3d level is clearly established. The strong-interaction effects increase from ^{16}O to ^{18}O by 74% ± 25% in shift and by 29% ± 12% in width.

Our results can be compared with theoretical calculations made by several authors [10–17], trying to fit previous $\bar{p}$-atom data. They are summarized in table 4 and displayed in fig. 3 in an ϵ–Γ plot for the 3d level of antiprotonic oxygen. As can be seen from this figure, nearly all theoretical values are at variance with our new data. This might be due to the fact that no precise experimental data on strong-interaction effects in antiprotonic atoms were available in the pre-LEAR period, leaving large uncertainties for theoretical models. Remarkable, however, is the good agreement between our data and the black-sphere model prediction [16] for the 3d width of $\bar{p}$–^{18}O.

Recently it was claimed that two families of $\bar{p}$-nucleus optical potentials [18] could reproduce $\bar{p}$-atomic data when analysing previous experimental results from antiprotonic C, O, S, and Y atoms [3,19]. These two families are shallow (S) potentials (strong real and weak imaginary part) and deep (D) ones (weak real and strong imaginary part). We have analysed our results from $\bar{p}$-^{16}O with an optical potential of the form $V^{opt} = -2\pi(1 + m_{\bar{p}}/M)A \cdot \varrho(r)/\mu$, where $m_{\bar{p}}$, M, and μ are the masses of the antiproton, of the ^{16}O nucleus, and the $\bar{p}$-^{16}O reduced mass. For the nuclear density we used the same distribution as in our earlier paper [3]. In the Re A-Im A plot of fig. 4 the values of A which reproduce our measured 3d shift (width) are shown by the horizontal (vertical) band. There exists only one solution which reproduces both quantities simultaneously. This plot also shows that an accurate determination of the shift (width) strongly fixes the imaginary (real) part of the optical potential. So the ambiguities as found by Ref. 18 are ruled out by our precise measurement of the strong-interaction effects in the 3d level of $\bar{p}$-^{16}O and the existence of a deep imaginary part is established. This is also supported by recent $\bar{p}$-nucleus scattering data [20].

The observation of the strong isotope effect in the antiprotonic oxygen isotopes provides a means of studying further details of the $\bar{p}$-nucleus potential, in particular the ratio of $\bar{p}p$ to $\bar{p}n$ interactions. From our spectra we can also derive the widths of the 4f and 5f levels, and the data are at present being evaluated. They will be used, together with the data given here, for a detailed analysis of the isotope effect to be published in a forthcoming paper.

5. SUMMARY AND CONCLUSIONS

We have reported on new measurements of strong-interaction effects in the stable antiprotonic oxygen isotopes. Shifts and widths of the 3d level are measured precisely. The strong-interaction effects increase from ^{16}O to ^{18}O by 74% in shift and 29% in width. Previous theoretical calculations fitted to the hitherto available experimental results hardly agree with our data, and further refinement of the theoretical approach is needed. The pronounced isotope effect indicates that the $\bar{p}n$ interaction is important, and/or that a neutron halo at least in ^{18}O plays an important role. A recent theoretical work claims that two families of optical models would reproduce $\bar{p}$-atomic data. This is ruled out by our $\bar{p}$-^{16}O measurement alone.

Acknowledgements

We would like to thank the LEAR staff for their extremely good collaboration during the test run and the final production runs for this experiment. Also, we wish to acknowledge the efforts of the design and construction departments of the KfK in the development of the experimental set-up. The work was supported by the Bundesministerium für Forschung und Technologie of the Federal Republic of Germany, the Schweizer Nationalfonds and the US National Science Foundation. We also thank H. Hagn, J. Hauth, E. Hechtl and P. Stoeckel for technical assistance.

REFERENCES

[1] H. Poth, Compilation of data from hadronic atoms, Physics Data Report No. 14-1 (1979), Fachinformationszentrum Karlsruhe.

[2] P. Lefèvre, D. Möhl and G. Plass, The CERN Low-Energy Antiproton Ring (LEAR Project), Proc. 11th Int. Conf. on High-Energy Accelerators, Geneva, 1980 (Birkhäuser, Basle, 1980), p. 819.

[3] H. Poth et al., Nucl. Phys. **A294** (1978) 435.

[4] Basle-Karlsruhe-Stockholm-Strasbourg-Thessaloniki Collaboration, CERN Proposal PS176, Study of X-ray and γ-ray spectra from antiprotonic atoms (spokesman H. Poth), CERN/PSCC/80-103 (1980). (Experiment in co-operation with PS 186.)

[5] H. Poth, Physics with antiprotonic atoms, Proc. Workshop on Physics with Low-Energy Cooled Antiprotons, Erice, 1982 (eds. U. Gastaldi and R. Klapisch) (Plenum Press, New York, 1984), p. 567.

[6] Th. Köhler, Thesis, University of Karlsruhe, KfK-Bericht, in preparation.

[7] U. Raich, Thesis, University of Karlsruhe, KfK-Bericht 3712 (1984).

[8] E. Borie and G. Rinker, Rev. Mod. Phys. **54** (1982) 67.
B. Jödicke, KfK-Bericht 3933, 1985.

[9] P. Barnes et al., Phys. Rev. Lett. **29** (1972) 1132.

[10] J.F. Haak, A. Lande and F. Iachello, Phys. Lett. **66B** (1977) 16.

[11] H. Nishimura and T. Fujita, Phys. Lett. **60B** (1976) 413.

[12] T. Suzuki and H. Narumi, Nucl. Phys. **A426** (1984) 413.

[13] A. Deloff and J. Law, Phys. Rev. **C10** (1974) 2657.

[14] O. Dumbrajs et al., in Proc. 3rd LEAR Workshop on Physics with Antiprotons in the ACOL ERA, Tignes, 1985 (eds. U. Gastaldi, R. Klapisch, J.M. Richard, J. Tran Thanh Van) (Editions Frontières, Gif-sur-Yvette, 1985), p. 569.

[15] A.M. Green and S. Wycech, Nucl. Phys. **A377** (1982) 441.
A.M. Green, W. Stepien-Rudzka and S. Wycech, Nucl. Phys. **A399** (1983) 307.

[16] W. Kaufmann and H. Pilkuhn, Phys. Lett. **62B** (1976) 165.

[17] D.A. Sparrow, Relativistic treatment of $\bar{p}$-atom shifts and widths, Preprint, University of Pennsylvania, Philadelphia, August 1985.

[18] C. Wong, A. Kerman, G. Satchler and A. MacKellar, Phys. Rev. **C29** (1984) 574.

[19] R. Roberson et al., Phys. Rev. **C16** (1977) 1945.

[20] D. Garreta et al., Phys. Lett. **135B** (1984) 266 and **139B** (1984) 464.

Table 1

Summary of PS176 beam time for oxygen measurement

Nucleus studied	Target	Spills	Stopped antiprotons
^{16}O	H_2O	4	295×10^6
^{17}O	H_2O	11	816×10^6
^{18}O	H_2O	9	578×10^6

Table 2

Results of the measurement of the strong interaction shifts ϵ and widths Γ (in eV) of the 3d level in the oxygen isotopes

Nucleus	Measured quantity	Value	Statistical error	Total error
^{16}O	ϵ	−112	3	20
	Γ	495	14	45
^{17}O	ϵ	−140	8	46
	Γ	540	26	150
^{18}O	ϵ	−195	5	20
	Γ	640	15	40

Table 3

Strong-interaction shifts and widths (in eV) of the 3d level in the oxygen isotopes

Target	Measured quantity	This experiment	Ref. [3]	Ref. [9]
^{16}O	ϵ	−112(20)	−124(36)	−60(73)
	Γ	495(45)	320(150)	648(150)
^{17}O	ϵ	−140(46)		
	Γ	540(150)		
^{18}O	ϵ	−195(20)	−189(42)	
	Γ	640(40)	550(240)	

Note: The shift ϵ is defined as the difference between the measured energy of the 4–3 transition and the calculated value assuming only electromagnetic interactions. The latter is 73.497 keV (^{16}O), 73.755 keV (^{17}O), and 73.985 keV (^{18}O).

Table 4

Shifts and widths of the 3d level of three oxygen atoms
First value: negative shift; second value: width (all in eV).

		^{16}O		^{17}O		^{18}O	
		$-\epsilon$	Γ	$-\epsilon$	Γ	$-\epsilon$	Γ
Experimental	Pre-LEAR *)	111(32)	480(110)			189(42)	550(240)
	LEAR	112(20)	495(45)	140(46)	540(150)	195(20)	640(40)
Theoretical [Ref.]	[10]	148	367				
	[11]	116	547				
	[12]	161	444			195	503
	[13]	134	578				
	[14]	125	652	155	858	181	750
	[15]	90	554			158	688
	[16]	–	532			–	646
	[17]	87	590				

*) Mean values

Figure captions

Fig. 1 X-ray spectra of $\bar{p}$-$^{16}O/^{17}O/^{18}O$.

Fig. 2 Fit results for the 4–3 line complex.

Fig. 3 Experimental results and theoretical fits to all previously available data for the shift and width of the 3d level in antiprotonic oxygen.
△ : Ref. 3; ○ : Ref. 9; ⊙ : Ref. 10; □ : Ref. 11; * : Ref. 12; + : Ref. 13; × : Ref. 14; ◇ : Ref. 15; ← : Ref. 16; ⊕ : Ref. 17; ● : this experiment.

Fig. 4 Optical model calculations for $\bar{p}$-^{16}O. Horizontal (vertical) band shows all values which reproduce the 3d level shift (width) from our measurement within the errors.

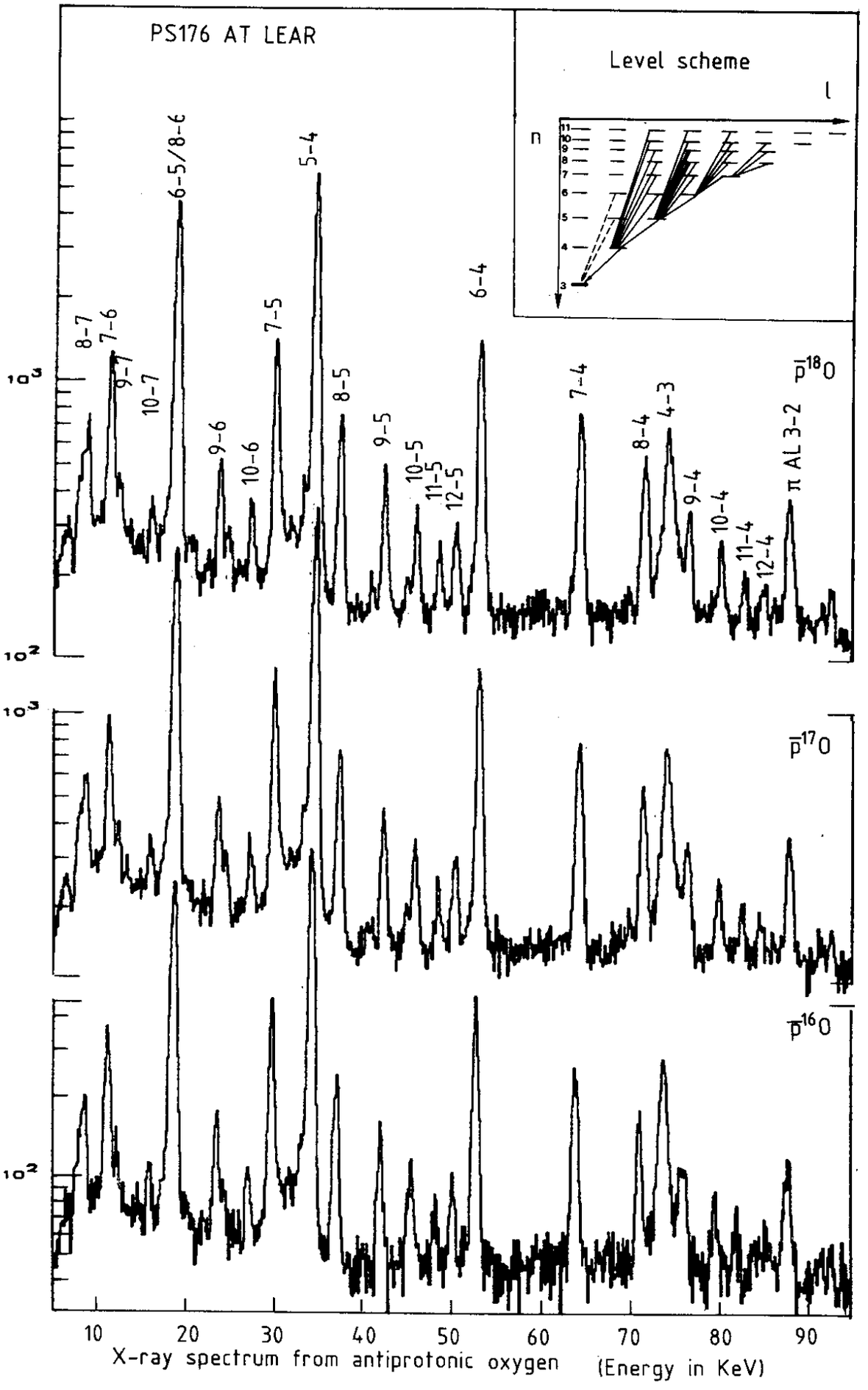
PS176 AT LEAR
Level scheme
n
l
$\bar{p}^{18}O$
$\bar{p}^{17}O$
$\bar{p}^{16}O$
8-7
7-6
9-7
10-7
6-5/8-6
9-6
10-6
7-5
5-4
8-5
9-5
10-5
11-5
12-5
6-4
7-4
8-4
4-3
9-4
10-4
11-4
12-4
π AL 3-2
10
20
30
40
50
60
70
80
90
X-ray spectrum from antiprotonic oxygen
(Energy in KeV)

Fig. 1

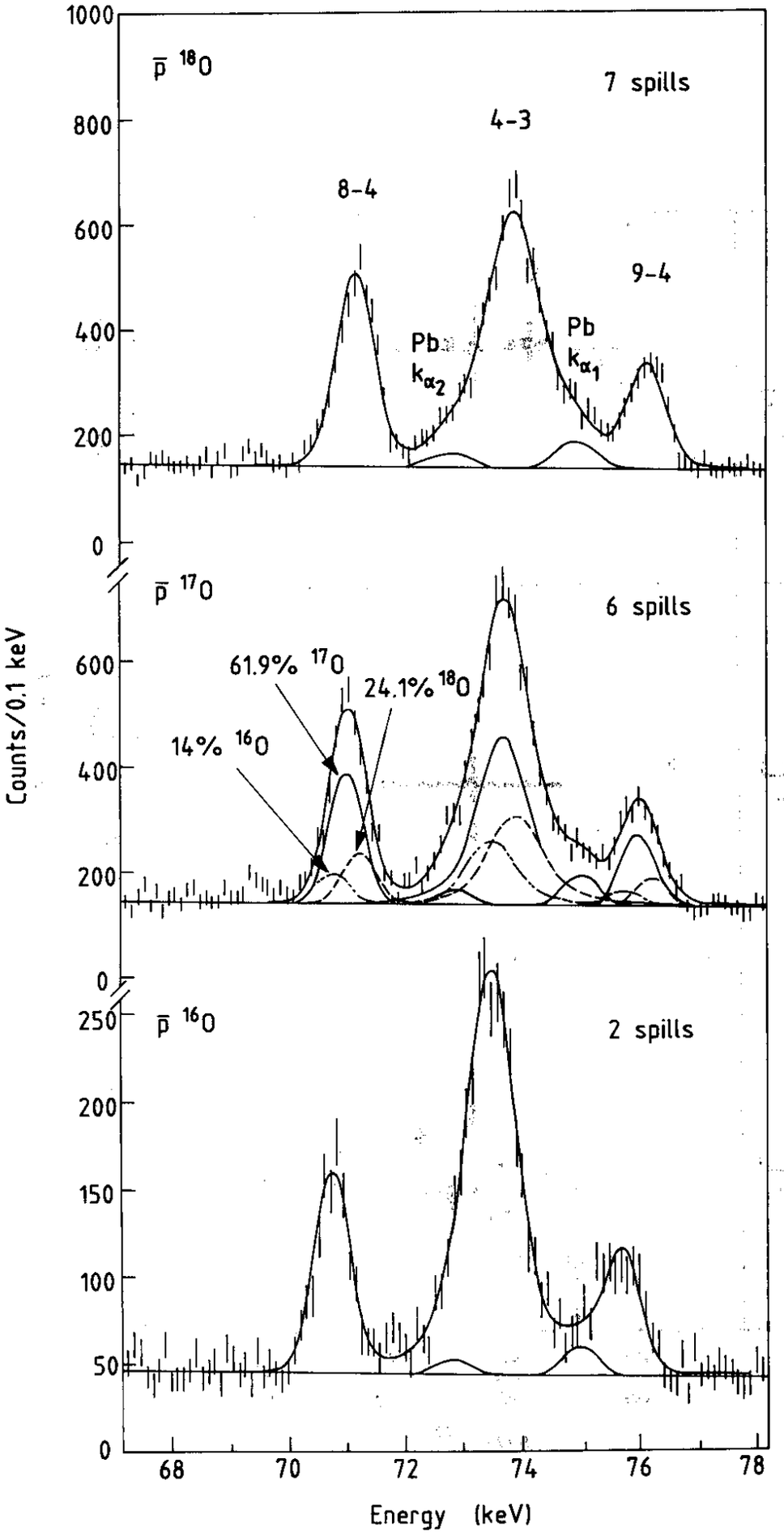
$\bar{p}$ ^{18}O
7 spills
4-3
8-4
9-4
Pb k_{α_2}
Pb k_{α_1}
$\bar{p}$ ^{17}O
6 spills
61.9% ^{17}O
24.1% ^{18}O
14% ^{16}O
$\bar{p}$ ^{16}O
2 spills
Counts/0.1 keV
Energy (keV)

Fig. 2

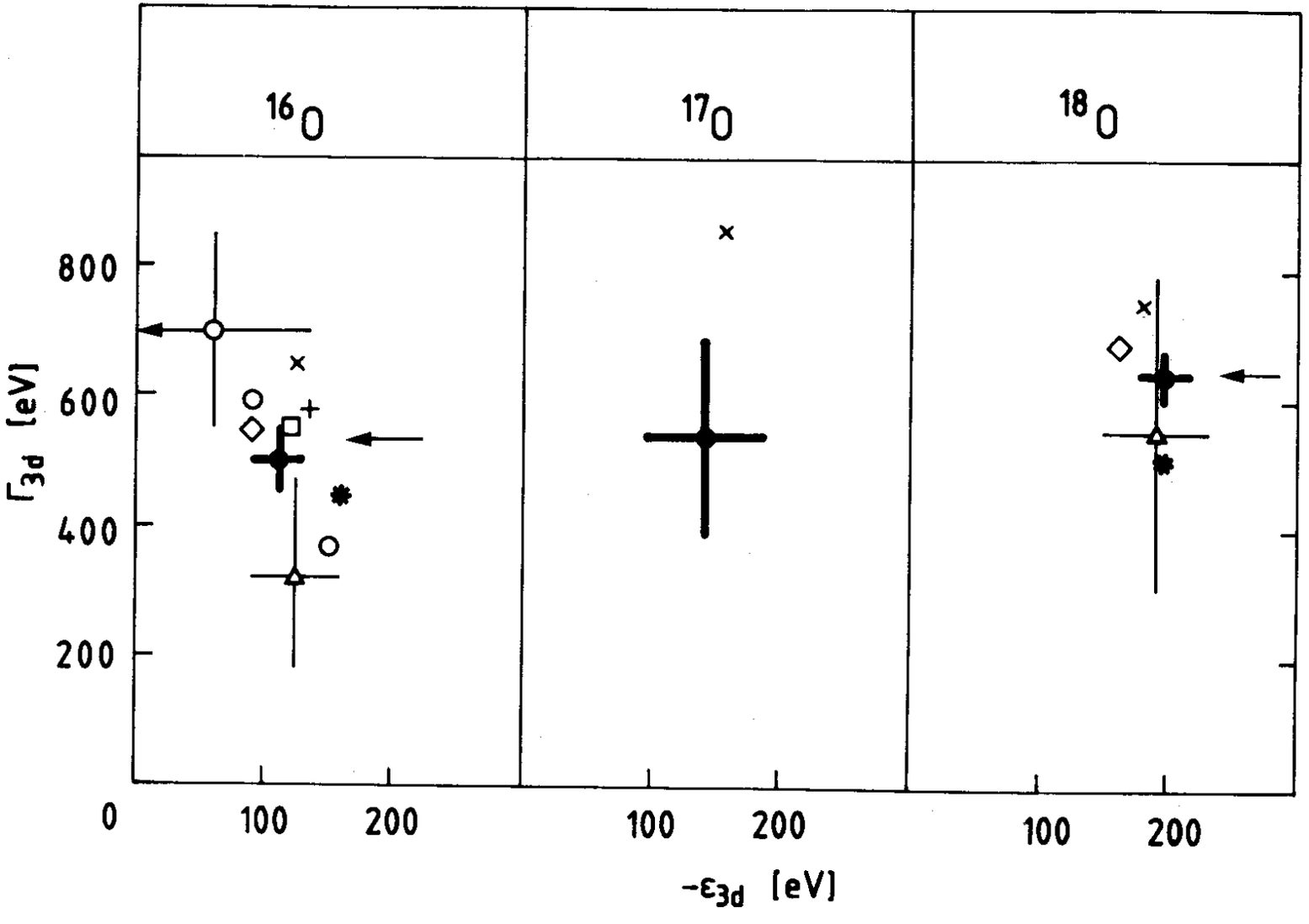
^{16}O
^{17}O
^{18}O
800
600
400
200
0
100
200
100
200
100
200
Γ_{3d} [eV]
$-\varepsilon_{3d}$ [eV]

Fig. 3

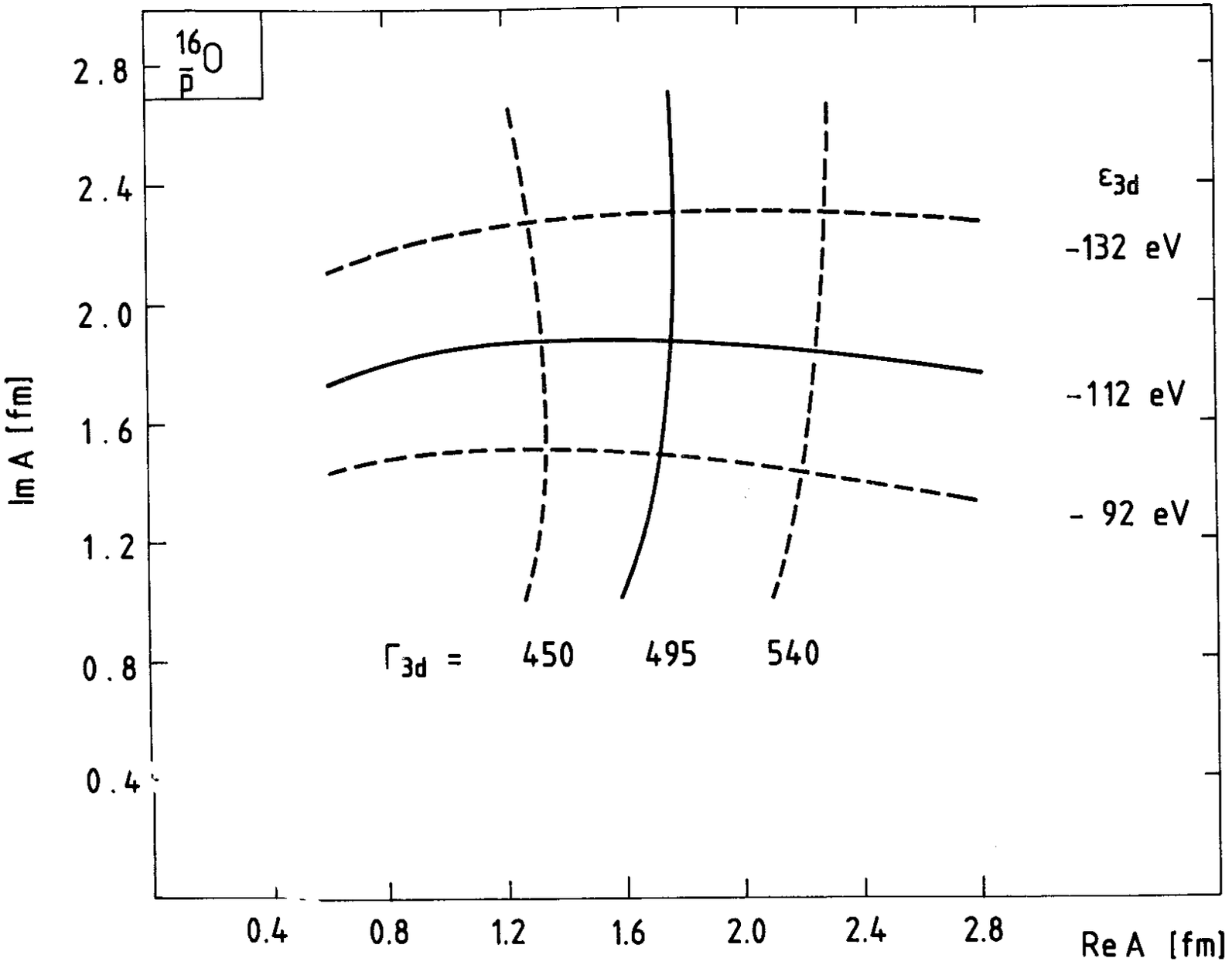
$^{16}_{\bar{p}}$O
2.8
2.4
2.0
1.6
1.2
0.8
0.4
Im A [fm]
ε_{3d}
-132 eV
-112 eV
- 92 eV
Γ_{3d} = 450 495 540
0.4 0.8 1.2 1.6 2.0 2.4 2.8
Re A [fm]

Fig. 4